Statistical studies of traveling ionospheric disturbances and equatorial plasma irregularities

Tal Sternberg [1,2] Shun-Rong Zhang [1] Ercha Aa [1]

[1]MIT Haystack Observatory [2]Dartmouth College

Abstract

This study provides a statistical analysis of both travelling ionospheric disturbances (TIDs) and equatorial plasma irregularities (EPIs) in the American sector as well as their potential correlation. The GNSS measurement of total electron content (TEC) from ground-based receiver networks were used to identify potential TIDs. A large global TID dataset based on ∼6000 GNSS receivers is being created at MIT Haystack Observatory for every day since 2018. Monthly averages of TID amplitudes with up to 1° latitude by 1° longitude by 5 min time interval spatial-temporal resolution are calculated. We have developed various visualization tools to assist in the characterization of TID climatology including day-to-day, seasonal, and long-term variations. To characterize EPIs, we use the GOLD's nightglow measurements at 135.6 nm. A statistical analysis for the EPI occurrence in the GOLD data is performed over the years since 2018, corresponding to the period of the GNSS TID climatology.

Background & Project Goals

Medium scale TIDs (MSTIDs) are regional with smaller wave lengths and shorter periodicity than large-scale TIDs originated in auroral zones. A significant TID source is terrestrial weather, which can generate gravity waves which then propagate upward into the ionosphere and thermosphere. Atmospheric disturbances and TIDs have been considered as necessary conditions to seed ionospheric irregularities at equatorial and low latitudes. Equatorial plasma irregularities (EPIs) associated with equatorial plasma bubbles result from ionospheric instability. EPIs occur during post-sunset in the ionosphere typically in regions of equatorial and low latitudes. EPIs can adversely affect the performance of navigation and communication systems, and their precise physical processes remain an active research frontier. This project will examine the statistics of MSTIDs and EPIs and whether EPIs are connected to MSTIDs.

- **Daily and Seasonal TID Variations** We will explore daily, monthly and yearly values of TID amplitudes (atec) in recent years (since 2019).
- **Daily and Seasonal EPI Variations** We will explore daily, monthly and yearly EPI occurrence corresponding to the period of TID statistics.
- **Correlation Between TIDs and EPIs** We will examine similarities in the yearly patterns of TIDs and EPIs and quantify their correlation.

Data and Methods

The primary data used for TID analysis are based on GNSS TEC observations from nearly 6000 GNSS receivers that have been collected and processed by MIT Haystack Observatory. Differential TEC (dTEC) values are further calculated by de-trending smooth background variations. The dTEC data are binned in latitude, longitude, and time for each of the individual days as well as months, therefore bin average amplitudes of dTEC are used to quantify TID activity. The EPI analysis is based on the geostationary observation by the NASA GOLD satellite providing the nightglow data at 135.6 nm wavelength (Figure 1). The GOLD data was filtered and processed to extract the EPI indices in a multi-step process described in the next section. This procedure was performed for every UT each night when GOLD data is available and therefore form a large EPI indice database for this study.

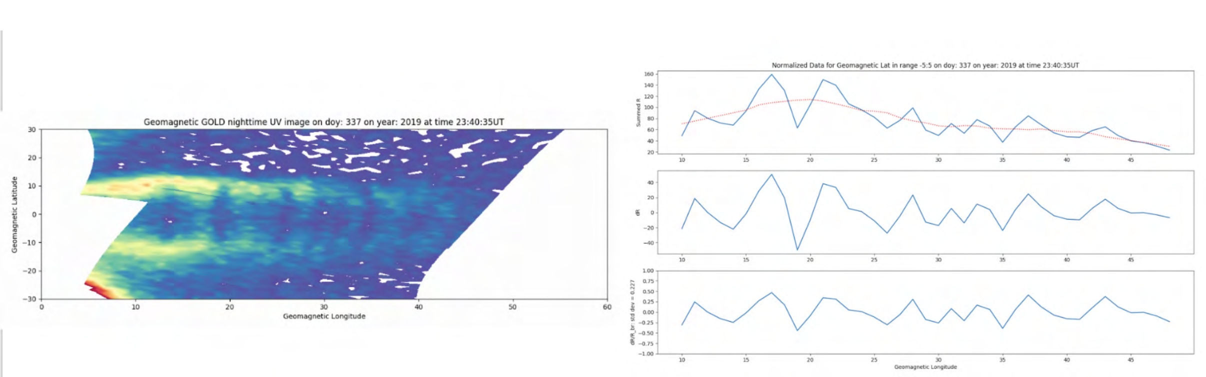

Figure 1. (LEFT) A graphical depiction of EPIs as shown by plotting GOLD data in a geomagnetic coordinate system at 23:40 UT on day 337 of year 2019 and (RIGHT) a graphical depiction of the process used to calculate EPI indexes

Results For TIDs and EPIs Seasonal Variation

TID seasonal variations were explored within individual months, and then years. These variations could be visualized using monthly average files or by iterating through every day in the year. As shown in the bottom of Figure 2, around 23-24 UT there is a clear seasonal variation of TIDs occurring more frequently in winter and fall and less frequently in spring and summer at this location -42.5°E, -2.5°N. This location was chosen for easy comparison with GOLD data and reasonable TID data availability. Because the geomagnetic coordinate range for the plotted GOLD data corresponded to a geographic coordinate range of -14.5∼-2.4°N geographic latitude and -62.5∼-27.3°E geographic longitude. After testing multiple permutations of these locations, -42.5°E -2.5°N appeared to have the best fit. These were also plotted month-to-month (top panel) to see monthly variations from documented terrestrial or space weather events.

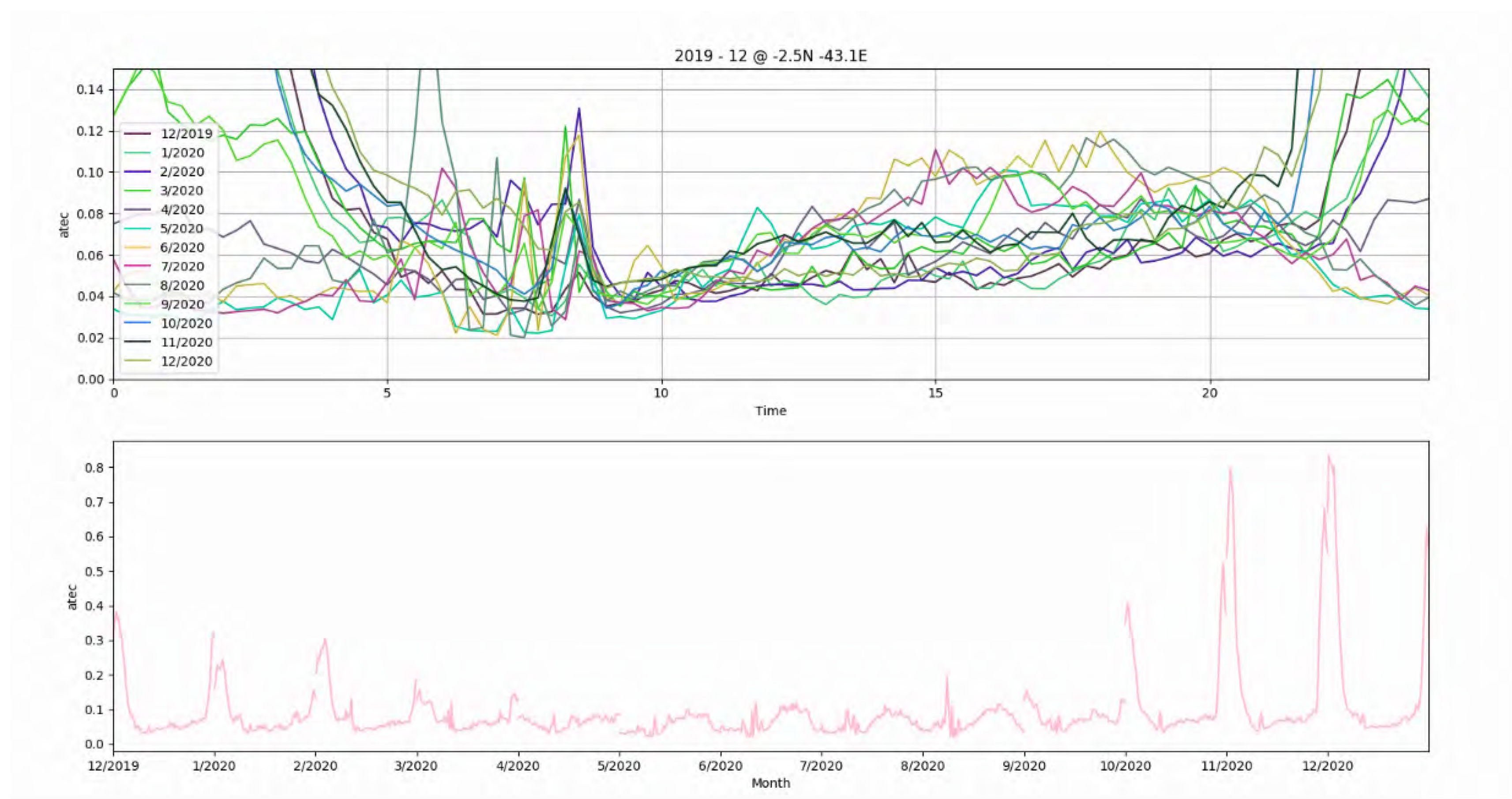

Figure 2. A year-long plot of the monthly average atec (TID amplitude) values for 12 months compared over 24 hours and chronologically

Next, EPI seasonal variations were viewed using GOLD data. Our program calculates the summed radiance over a specified latitude range for each of the longitude grids at a given UT, the background radiance, and the standard deviation of difference between background radiance and summed radiance over the background. This specified latitude range is -5 to 5°N magnetic latitudes in order to characterize the EPIs. Indicators of EPIs were points with high standard deviations of the change in radiance over the background radiance of near-equator latitudes. There is a subtle pattern of weaker irregularity indexes in the spring and summer months as compared to higher values of those in the fall and winter. These were also plotted month-to-month to see monthly variations.

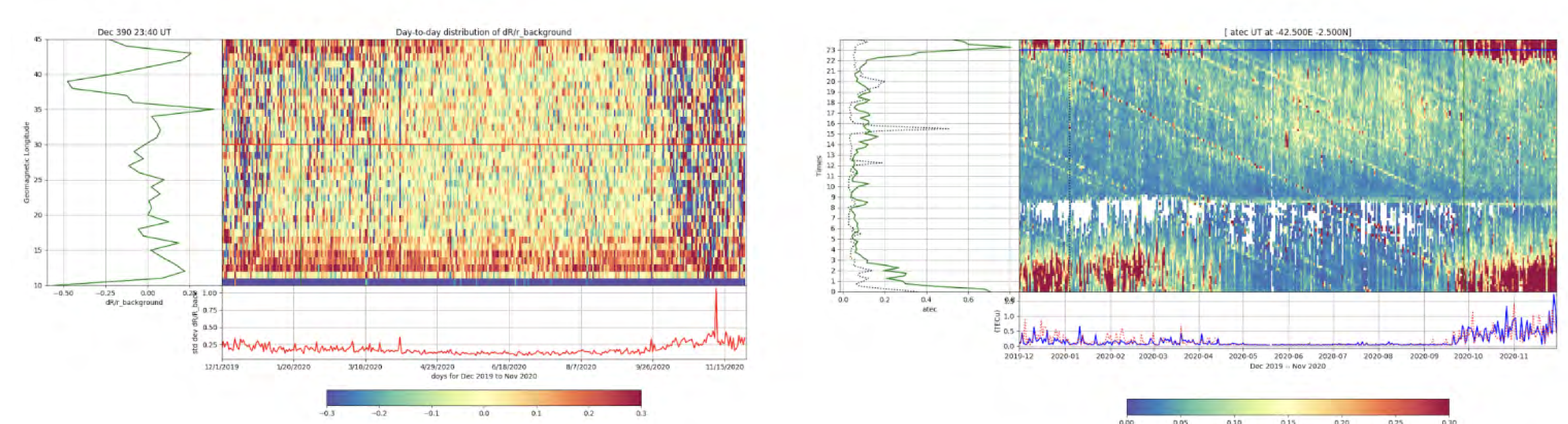

Figure 3. (LEFT) A year-long contour plot of dR/Rback values at 23:40 UT varying by date and geomagnetic longitude and (RIGHT) a year-long contour plot of atec values as a function of date and UT

Results for Correlation Between TIDs and EPIs

Based on previous hypotheses and the similar seasonal patters of TIDs and EPIs as demonstrated in Figure 3, it is worthwhile to quantify the correlation between the TID index (the averaged dTEC) and the EPI index (the standard deviation of the differential radiance divided by the background trend). To do this, we combined GNSS and GOLD data and plotted the TID index against the EPI (Figure 4). We used a TID index at -42.5°E -2.5°N at time 23 UT and corresponding EPIs at 23:40 UT to account for possible time lag between TIDs and EPIs.

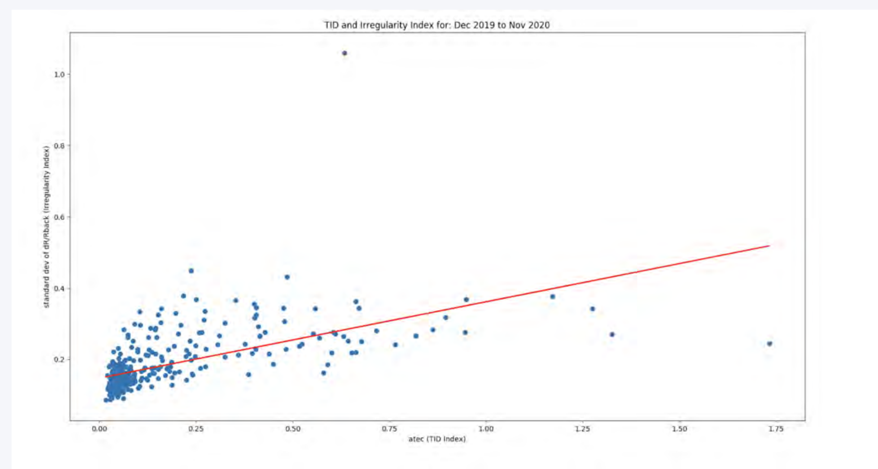

Figure 4. Every point represents the TID index and EPI index of a day in the year from dec 2019 - nov 2020

The data had a Pearson's (linear) correlation of 0.580 at -42.5°E -2.5°N at 23:00 UT, indicating a subtle positive linear correlation. Using TIDs at 23:00 UT and EPIs at 23:40 UT mitigates against a likely lag time between the TIDs and EPIs. This result strengthens the hypothesis that TIDs are connected to the formation of EPIs in the ionosphere. Month-to-month correlations also have a positive trend on average as shown in Figure 3.

Summary

This study provides results of seasonal variations for TIDs which demonstrate a steady trend of higher TID activity being captured in January-April and October-December with a quieter period during May-September. NASA's GOLD Mission's data provides EPI index values at the magnetic equator that also appear to vary on the same trend. By using year-long (Dec 2019-2020) nearly simultaneous TID and EPI index data, a scatter plot shows a positive linear correlation between the two phenomena. Further analysis needs to be done on a longer time span of the datasets from multiple locations to strengthen this assertion and perhaps different statistical models can be run and compared to initial results. A further understanding of this relationship may lead to a more comprehensive view of the impact of space and terrestrial weather on the ionospheric irregularity and perhaps eventually result in forecasts or projections in an appropriate time window.

References

Aa, et al. (2019). Coordinated ground-based and space-based observations of equatorial plasma bubbles. JGR: Space Physics, 2019JA027569.

Hunsucker, R. D. (1982). Atmospheric gravity waves generated in the high-latitude ionosphere: A review. Reviews of Geophysics, 20(2), 293–315.

Rideout, W., & Coster, A. (2006). Automated GPS processing for global total electron content data. GPS Solutions, 10(3), 219–228.

Vierinen, et al. (2015). Statistical framework for estimating GNSS bias. Atmospheric Measurement Techniques Discussions, 8(9), 9373–9398.

Zhang et al. (2017). Ionospheric Bow Waves and Perturbations Induced by the 21 August 2017 Solar Eclipse. Geophysical Research Letters, 44(24), 12–067–12–073.